

IMEKO 2010 TC3, TC5 and TC22 Conferences
Metrology in Modern Context
November 22–25, 2010, Pattaya, Chonburi, Thailand

AN INVESTIGATION INTO DEPTH SENSING OF HARDNESS MAPS BY MEANS OF IMAGE PROCESSING TECHNIQUES

*Malek Naderi*¹, *Kasra Sardashti*², *Ali Sharbatian*³, *Mehdi Iranmanesh*⁴

¹ Department of Mining and Metallurgy, Amirkabir University of Technology, Tehran, Iran,
m.naderi@aut.ac.ir

² Department of Mining and Metallurgy, Amirkabir University of Technology, Tehran, Iran,
kasra.sardashti@gmail.com

³ Department of Mining and Metallurgy, Amirkabir University of Technology, Tehran, Iran,
a.sharbatian@gmail.com

⁴ Department of Marine Sciences and Ship Engineering, Amirkabir University of Technology, Tehran, Iran, iranmanesh@aut.ac.ir

Abstract - Depth sensing is a novel technique to obtain useful information about mechanical properties of materials. To measure depth of indents, two methods can be employed: in situ depth sensing and residual penetration depth sensing. In this paper, a novel image processing technique is utilized by authors to estimate depth of residual indents, made by a scanning hardness tester. In this quick and simple technique, instead of using depth sensing instruments, microscopic images of scanned areas were analyzed by image analysis software. The profiles of light intensity obtained by the software were correlated by the hardness values and consequently penetration depths. The depth values obtained were in complete agreement with standard depth given for certain values of Vickers hardness.

Keywords: Depth sensing; Hardness map; Image processing;

1. INTRODUCTION

Depth of impressions made during hardness testing indentation, may contain useful information about mechanical behavior and distribution of phases, on surface of various materials. This concept was first to be mentioned by the depth sensing indentation method in 1983.

This technique is based on high – resolution instruments that continuously monitor the loads and displacements of an indenter as it is pushed into and withdrawn from a material. Load – penetration depth curves are the most valuable data obtained by this method, which can reveal useful information about elastic and plastic deformation [1], fatigue and creep of materials evaluated [2]. The most common properties that depth sensing methods provide are the elastic modulus and hardness [3]. Hardness values are obtained from the elastic displacement occurred, during the indentation.

However, such techniques require accurate displacement measurements of the indenter, during loading and unloading. Thus, in situ depth measurements i.e. load-penetration curve monitoring [2] suggested to be replaced by, scanning residual impressions remained after test loading and subsequent unloading [4]. This method coupled with a hardness mapping technique [5] could provide distribution of possible phases on surface of the test piece.

Objective of the present work was to determine depth of the indents produced during scanning hardness measurement, by means of a simple and quick image analysis procedure, and correlate the data obtained with hardness values measured.

2. EXPERIMENTAL: MATERIALS AND METHODS

A 321 stainless steel block with 4 cm² side area, was grinded and polished by conventional metallographic methods. The sample's hardness was firstly measured by routine Vickers hardness testing method. The sample was then tested by a hardness mapping technique, developed in Hamyar Sanat Eghbal Co. In this technique, the surface of the sample was scanned, using an indenter applying a 10 N force on the surface, and recorded the hardness values on Vickers scale.

The indenter scanning areas had square shapes with hundred indented points. The distance between points varies in different scanning areas, and had values 0.2mm and 0.3mm. Conventional photography cameras were used to take pictures from scanning zones on the sample. These scanned areas were then examined by light microscope and images of various series of indents were taken in ×40 magnification. Some of the scanning zones were also evaluated by scanning electron microscope (SEM) images.

These images were analyzed in the image analysis software and profiles of light intensity were obtained. Intensity maps were correlated with the hardness quantities measured by the testing machine and their corresponding depths of penetration.

3. RESULTS AND DISCUSSION

Hardness values vary in different points of scanning zones with various indent distances. Table.1 shows the hardness values obtained in a square scanned zone with indent distance of 0.2mm. Variation in hardness magnitudes is also illustrated in form of contour graphs, as illustrated in Fig.1.

Table 1.Hardness magnitudes in a 10×10 points scanning surface. Distance between indents = 0.2mm

HARDNESS VALUES (HV10)									
383	367	386	385	380	391	384	388	383	357
369	392	371	380	348	380	366	382	371	361
377	370	375	386	381	385	354	384	370	412
384	370	385	355	381	366	356	398	367	391
388	391	387	334	389	392	373	395	360	391
383	367	380	377	377	402	378	398	382	367
385	357	384	396	402	396	378	409	383	384
368	361	389	396	411	385	395	382	383	374
347	363	385	357	399	393	406	381	378	385
363	357	367	392	383	383	401	353	393	370

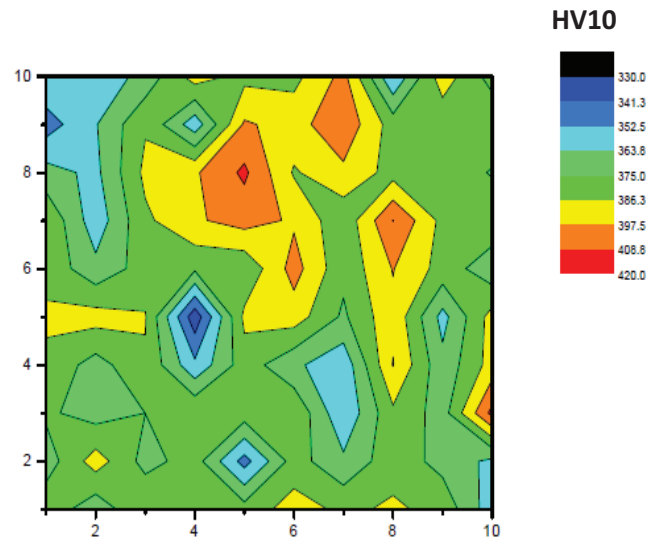


Fig.1 Contour map for hardness values resulted from hardness testing with indentation distance of 0.2 mm.

As can be seen in Fig.1, hardness varies significantly in the scanning surface. The maximum hardness value obtained is 412 HV while the minimum is 334 HV.

In Table.2, hardness quantities for indentation distance of 0.3 mm are presented. In addition, Fig.2 is the contour graph of hardness values for 100 indentation points.

Table 2. Hardness magnitudes for a 10 × 10 scanning surface.
Distance between indents = 0.3mm

HARDNESS VALUES (HV10)									
403	420	403	388	374	378	374	368	377	380
434	403	392	377	399	391	363	366	357	394
458	397	385	372	371	395	360	393	374	406
464	389	399	378	357	380	388	373	364	395
439	388	386	394	379	386	367	356	394	361
463	397	402	390	369	386	385	367	388	356
442	394	391	392	403	360	372	356	394	360
456	386	396	378	410	377	363	391	369	370
457	394	401	376	363	368	348	377	388	392
417	394	390	376	375	381	378	367	403	402

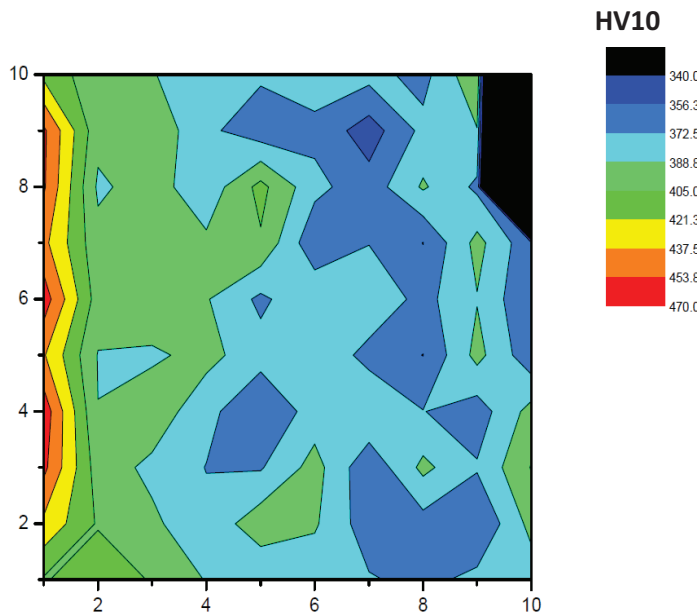


Fig.2 Contour map for hardness values resulted from hardness testing with indentation distance of 0.3 mm.

According to Table.2, the maximum hardness magnitude measured is 457 HV and the minimum magnitude is 348 HV. Thus, variations in hardness seem to be more significant when the distance between indents is 0.3 mm. Also, the area with hardness values more than 380 HV is higher for 0.3mm indent distance. However, in accordance

with Fig.2, points with hardness higher than 400 HV are concentrated to the left side of the map and hardness mostly varies between 330 and 400 HV, as also seen for indentation distance of 0.2mm.

SEM and light microscope images of a series of indentation points in a scanning zone, including twelve points for indentation distance of 0.3mm, are shown in Fig. 3. Some images were also taken from the scanning zones, utilizing conventional photography cameras. In these pictures (Fig.4), change in light intensity inside the indents is much more pronounced, than microscopic micrographs. Therefore, scanning zones pictures, taken by cameras were analyzed by the image processing software and profiles and contour graphs of indentation depth in different points were obtained.

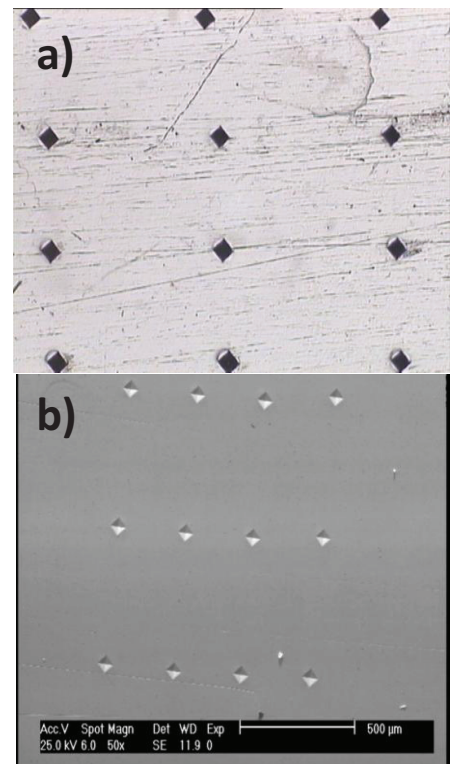


Fig.3 Microscope images of indentation points of a scanning area including 12 points with 0.3mm in distance, taken by (a) light microscope (×40), (b) SEM (×50).

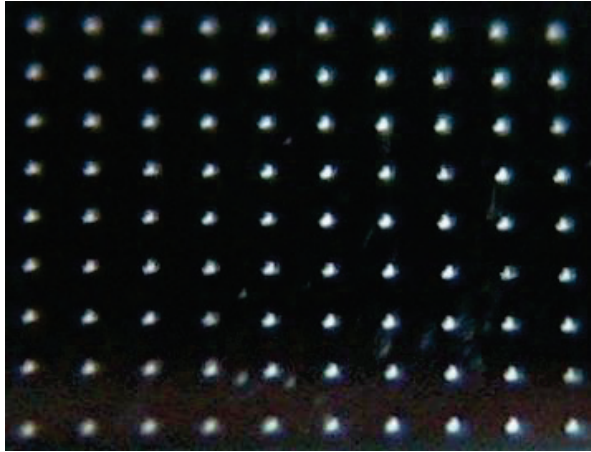


Fig.4 Image of scanning area of 90 indentation points with 0.3 mm distance, obtained by conventional digital photography camera.

In Fig.5, results of analysis for some indentation points in Fig.4 are shown in the form of contour and line profile graphs. The graphs are drawn on the basis of light intensities observed for the image. Light intensity of grayscale pictures is assigned to vary from 0 (black) to 260 (white). The amount of intensity also changes along the indent slant surfaces. These changes are the sources of formation of contour lines inside the indentation marks.

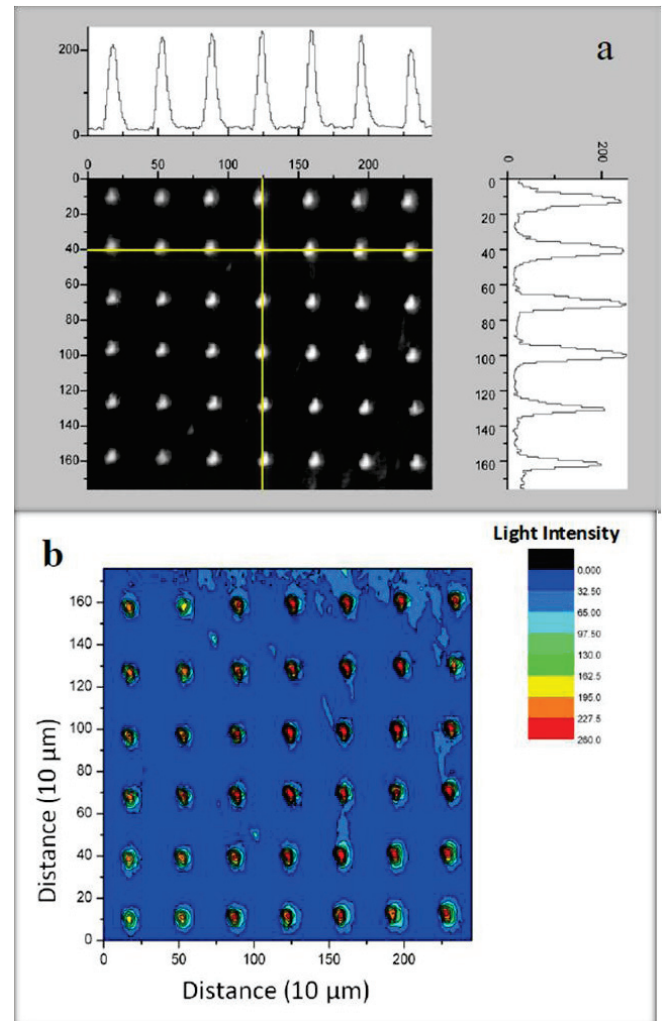


Fig.5. (a) Light intensity profiles of two perpendicular lines of indentation points, (b) Contour graph of light intensity, in a scanning area with 100 points with 0.3mm in distance.

Due to different standards, several relations between hardness and penetration depth have been defined. One of these standards is ASTM A1038, which is defined for indentation load of 10N [6]. The corresponding hardness – depth equation is as follows:

$$d = 0.062 \times \sqrt{\frac{F}{HV}} \quad (1)$$

, wherein F is the indentation load in N, d is penetration depth in mm and HV is magnitude of Vickers hardness. Also, it must be noted that, as a rule, the thickness of the sample should be higher than the minimum of ten times the indentation depth.

Regarding the hardness – depth relation, the values for hardness given in Table.1 and 2 can be converted to penetration depths, which are presented in Table.3 and Table.4, for the two different testing distances.

Table 3. Penetration depth for scanning distance of 0.2 mm.

Depth (micrometer)									
10.018	10.234	9.979	9.992	10.058	9.915	10.005	9.954	10.018	10.377
10.207	9.903	10.179	10.058	10.51	10.058	10.248	10.031	10.179	10.319
10.098	10.193	10.125	9.979	10.045	9.992	10.421	10.005	10.193	9.659
10.005	10.193	9.992	10.406	10.045	10.248	10.391	9.828	10.234	9.915
9.954	9.915	9.966	10.728	9.941	9.903	10.152	9.865	10.333	9.915
10.018	10.234	10.058	10.098	10.098	9.779	10.084	9.828	10.031	10.234
9.992	10.377	10.005	9.852	9.779	9.852	10.084	9.695	10.018	10.005
10.22	10.319	9.941	9.852	9.671	9.992	9.865	10.031	10.018	10.138
10.525	10.291	9.992	10.377	9.815	9.89	9.73	10.045	10.084	9.992
10.291	10.377	10.234	9.903	10.018	10.018	9.791	10.435	9.89	10.193

Table 4. Penetration depth for scanning distance of 0.3 mm.

Depth (micrometer)									
9.767	9.567	9.767	9.954	10.138	10.084	10.138	10.22	10.098	10.058
9.411	9.767	9.903	10.098	9.815	9.915	10.291	10.248	10.377	9.877
9.161	9.84	9.992	10.165	10.179	9.865	10.333	9.89	10.138	9.73
9.102	9.941	9.815	10.084	10.377	10.058	9.954	10.152	10.276	9.865
9.357	9.954	9.979	9.877	10.071	9.979	10.234	10.391	9.877	10.319
9.112	9.84	9.779	9.928	10.207	9.979	9.992	10.234	9.954	10.391
9.326	9.877	9.915	9.903	9.767	10.333	10.165	10.391	9.877	10.333
9.181	9.979	9.852	10.084	9.683	10.098	10.291	9.915	10.207	10.193
9.171	9.877	9.791	10.111	10.291	10.22	10.51	10.098	9.954	9.903
9.601	9.877	9.928	10.111	10.125	10.045	10.084	10.234	9.767	9.779

According to the tables 3 and 4, for the two indentation intervals of 0.2 mm and 0.3 mm, contour maps of penetration depth extents can be drawn (Fig.6 and Fig.7). These maps are also illustrated in a 3D form in Fig.8 and Fig.9.

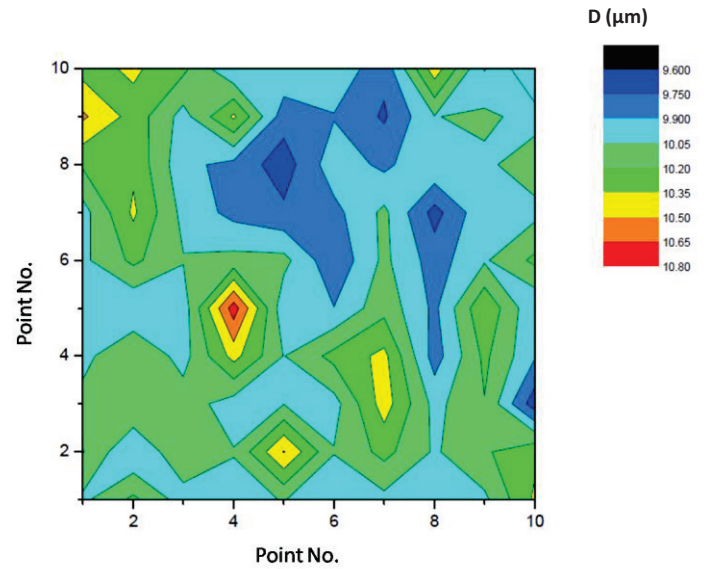


Fig.6 Penetration depth 2D map for indentation distance of 0.2 mm.

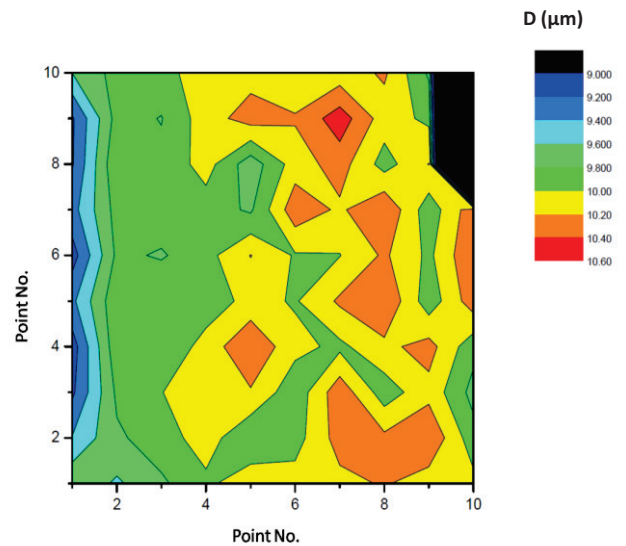


Fig 7. Penetration depth 2D map for indentation distance of 0.3 mm.

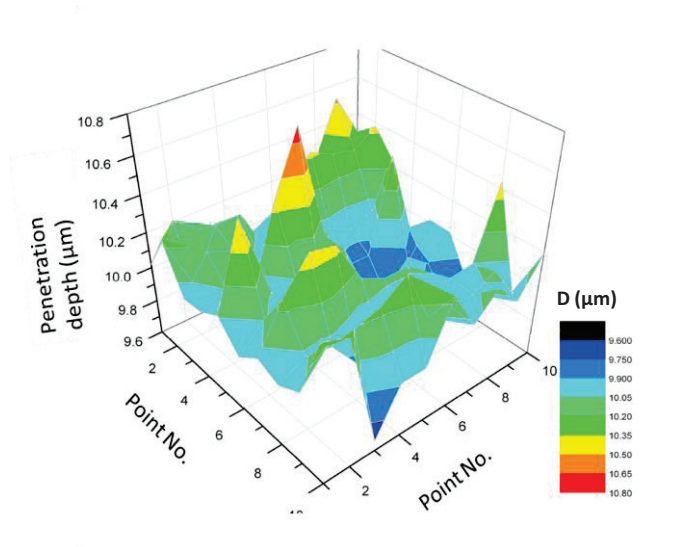


Fig.8 3D map for penetration depth in hardness testing with distance of 0.2 mm.

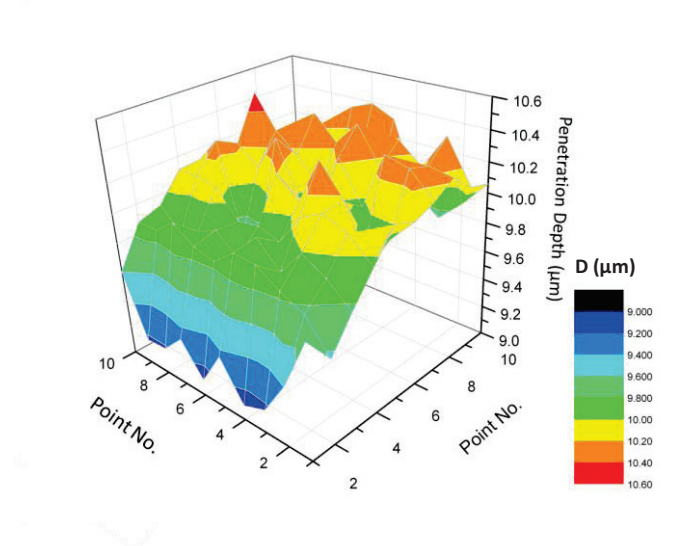


Fig 9. 3D map for penetration depth in hardness testing with distance of 0.3 mm.

The 2D and 3D contour maps are similar to those drawn for hardness values. These maps and the values given in the tables 3 and 4 are correlated with the level of light intensity obtained from the images. With the correlation referred, the color legend given in Fig.5 can be rewritten in terms of penetration depth. The resultant contour map is illustrated in Fig.10.

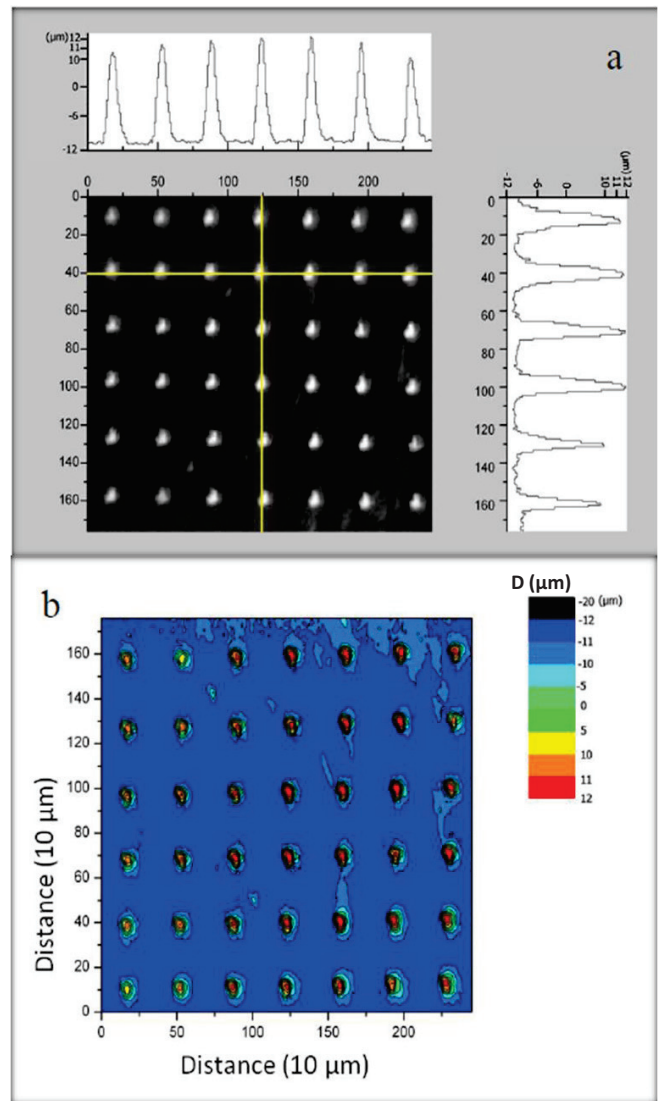


Fig.10. (a) Depth profiles of two perpendicular lines of indentation points, (b) Contour graph of indentation depth, in a scanning area with 100 points with 0.3mm in distance.

Change in depth along the slant surfaces of the indents can be determined with regard to the indenter geometry. The gradual change in depth along these oblique surfaces can be observed in term of light intensity contour lines. Therefore, variations of indentation depth in two perpendicular lines of a 10×10 points scanning area are plotted in Fig. 10 (a). It is observed on the profiles that along a certain line of scanning, depth of indents vary and this is in agreement with variation of hardness values in diverse testing points.

4. CONCLUSION

In this manuscript, a simple and quick approach to estimate depth of residual impressions resulted from hardness indentation testing is suggested. With regard to resultant depth profiles and graphs in this technique, it is concluded that:

Preparing clear microscopic images of areas scanned by scanning hardness testing machine and analyze them with proper image processing software, can result in acceptable estimation of indentation depth which is in agreement with standard depth for certain hardness values.

ACKNOWLEDGEMENT

The authors wish to thank to Poshteban M. Eng and Naderi M. Eng of Hamyar Sanat Eghbal Co. for their suggestions and supports in performing the hardness measurements by scanning hardness machine.

REFERENCES

- [1] M.F. Doerner and W.D. Nix, A method for interpreting the data from depth sensing indentation instruments, *Journal of Materials Research*, Vol.1, No.4 (1986) 601-609.
- [2] Zhi-Hui Xu , *Mechanical Characterisation of Coatings and Composites- Depth Sensing Indentation and Finite Element Modelling*, Ph. D. Thesis, MSE, KTH, 2004, P.5.
- [3] J. Gubicza, A. Juh'asz, and J. Lendvai, A new method for hardness determination from depth sensing indentation tests, *Journal of Materials Research*, Vol.11, No.12 (1996) 2964-2967.
- [4] D. Yang, T. J. Wyrobek, US Patent 2005/0283985 A1.
- [5] M. Naderi, A. Saeed-Akbari, W. Bleck, The effect of non-isothermal deformation on martensitic transformation in 22MnB5 steel, *Materials Science and Engineering A* 487 (2008) 445-455.
- [6] ASTM Standard A1038, "Standard Practice for Portable Hardness Testing by the Ultrasonic Contact Impedance Method".